Fiber stacking sequence effects on impact damage dimensions

Le Thi Tuyet Nhung[1,#] and Nguyen The Hoang[2*]

1 Department of Aerospace Engineering, Hanoi University of Science and Technology, Viet Nam
2 Faculty of Aviation Engineering, Vietnam Aviation Academy, Viet Nam
Corresponding Author Emails : nhung.lethituyet@hust.edu.vn, *hoangnt@vaa.edu.vn

KEYWORDS: Composite, Impact damage, Delamination, Fiber stacking sequence

Predicting impact behavior on composite plate is important for application into real products. Using numerical simulation method (ABAQUS), damage initiation and damage propagation can be observed, evaluated and analyzed. However, the proposed model needs validating with experimental results to ensure the accuracy of simulations. It is employed by comparing with results of papers using models without cohesive elements [2,3]. Firstly, the impact simulation was carried out on a 16 ply-crossply $[0_4/90_4]_S$ CFRP. The composite plate has a circular shape subjected by the impact of a steel ball falling down without initial velocity from a given height. The material properties are taken from the specimens used in the litterature. After that, a cohesive zone is attached into the interfaces of the composite plate to model delamination phenomenon and to determine the best optimized fiber direction against impact among $[0_4/15_4]_S$, $[0_4/30_4]_S$, $[0_4/45_4]_S$, $[0_4/60_4]_S$ and $[0_4/90_4]_S$ configurations and for different levels of impact energy. It is shown that the delamination shape obtained from the numerical model is similar to the experimental work. It has also been revealed that damage dimensions are maximum for $[0_4/45_4]_S$ and minimum for $[0_4/90_4]_S$.

Manuscript received: September, 2021 / Revised: January 01, 2022 / Accepted: February 15, 2022

NOMENCLATURE

D_m = Damage of the matrix
D_f = Damage of the fiber
D_d = Damage due to demalination

1. Introduction

Composite materials are more and more used because of their high strength-to-weight and stiffness-to-weight ratios. More specifically, the use of fiber composite laminated structures regularly increases, in particular in high performance situations, such as in aerospace and advanced transport industries. The usage of advanced composite materials in recent modern commercial aircraft has been increased up to 50% (**Figure 1**) or more of its total weight.

However, damage mechanism and the influence of damage types in composites on its properties are extremely complex. **Figure 2** shows some typical damage modes found in a composite laminate under a loading condition, which could include: Matrix cracks, delamination between layers, fiber-matrix debonding or fiber fracture.

Composite laminates generally have low impact strength because of their low transverse and interlaminar shear strength. A good understanding of impact-induced damage and failure of composite materials is vital for a reliable structural design. Many researchers built experiments to observe impact process (gas gun test, drop-weight test…), but these require expensive time and budget. Then, with the development of digital super computers, numerical simulation methods have been used to predict impact behavior on composites. An intensive review of research on impact damage is found in recent literature [1].

R.K. Luo et al. investigated a method with three failure criteria calculated on a solid element structure [2,3]. This approach predicted whether the structure is damaged or not and give a good idea of the geometry of damages. F. Aymerich et al. studied the potential of cohesive interface elements for damage prediction in laminates [4]. Their model gave correct simulation of the impact response of laminates in a wide range of energy values and successfully predicted size, shape and location of main damage mechanisms.

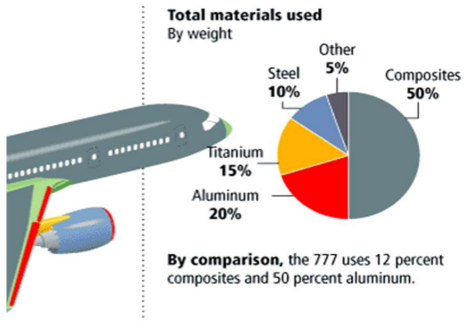

Fig.1 Materials used to construct the Boeing 787 Dreamliner [7]

R.K. Luo et al. investigated a method with three failure criteria calculated on a solid element structure [2,3]. This approach predicted whether the structure is damaged or not and give a good idea of the geometry of damages. F. Aymerich et al. studied the potential of cohesive interface elements for damage prediction in laminates [4]. Their model gave correct simulation of the impact response of laminates in a wide range of energy values and successfully predicted size, shape and location of main damage mechanisms.

The work reported here is to determine the best optimized fiber stacking sequence on a 16 ply-crossply $[0_4/\alpha_4]_S$ CFRP where the values of α are successively 90, 60, 45, 30 and 15 degrees.

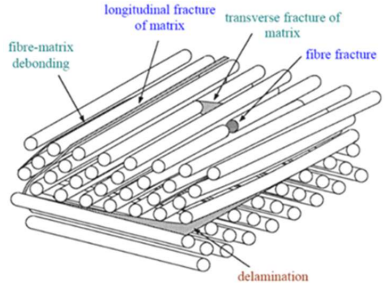

Fig.2 Damage modes in composite laminates

2. Simulation and results

2.1 Finite element model

The composite structures studied in this paper was a [04/904] s CFRP circular plate. Every ply thickness was included between 0.13 and 0.14 mm. So, 0.135 mm was chosen as the average thickness of each ply. Because of the symmetry of the circular plate, just a quarter of the plate was created in the finite element model as shown in Figure 3.

A three-dimensional (3D) Finite Element model, using ABAQUS CAE package, has been developed to simulate and evaluate damage. Three damage modes including matrix cracking, delamination and fiber failure have been assessed. Since they have only two interfaces, three layers of elements are arranged through the thickness. To model the circular composite plate, the eight-node brick elements with reduced integration C3D8R were employed. And to model the potential interaction area between the steel ball and the plate, the six-node wedge elements C3D6 were used. The total number of elements was 5947 and the total number of nodes was 8172. The steel ball was modeled as a rigid body. To define the interaction between the impactor and the plate, the steel ball surface was defined as a 'master surface' and the plate surface as a 'slave surface'. The damping ratio used to define the interaction was 0.0152 as determined by R.K. Luo et al. [2] (see Table 1). Material properties are defined in table 1 and come from R.K. Luo et al.'s work.

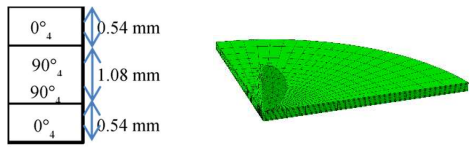

Fig.3 Illustration of the laminate thickness & quarter plate finite element model

2.2 Failure criteria

Results were compared with results from R.K. Luo et al.'s paper [3]. For this reason, the three same failure modes, matrix failure, delamination and fiber breakage were considered. These three failure criteria were not implemented in a program but used with a spreadsheet. So, values were picked up one by one from ABAQUS results.

2.2.1 Matrix failure

The matrix is considered failed if the following criterion is reached:

$$D_m = \left(\frac{\sigma_{22}}{[\sigma_{22}]}\right)^2 + \left(\frac{\tau_{12}}{[\tau]}\right)^2 + \left(\frac{\tau_{23}}{[\tau]}\right)^2 \geq 1 \qquad (1)$$

All stress components (σ22, τ12 and τ23) on a potential fracture plane (1-0-3) are included in Equation 1. This equation describes an ellipsoidal failure envelope (given a value of the right hand side equal to unit). Any point inside the envelope shows no failure in the material.

Table 1 Mechanical properties of laminates

E_{11} (GPa)	145
E_{22}, E_{33} (GPa)	9.2
G_{12} (GPa)	4.6
G_{13} (GPa)	5.2
G_{23} (GPa)	3.0
γ_{12},γ_{13}, γ_{23}	0.3
$[\sigma_{11}]$ (MPa)	2500
$[\sigma_{22}]$, $[\sigma_{33}]$ (MPa)	56
$[\tau]$ (MPa)	50
ρ (kg/m³)	1600
ξ	0.0152

2.2.2 Interlaminar delamination

Delamination appears when the following criterion is reached:

$$D_d = \left(\frac{\sigma_{33}}{[\sigma_{33}]}\right)^2 + \left(\frac{\tau_{13}}{[\tau]}\right)^2 + \left(\frac{\tau_{23}}{[\tau]}\right)^2 \geq 1 \qquad (2)$$

This failure criterion includes all stress components (σ33, τ13 and τ23) on a potential fracture plane (1-0-2). Equation 2**Error! Reference source not found.** describes an ellipsoidal failure envelope (given a value of the right hand side equal to unity).Any point inside the envelope shows no failure in the material.

2.2.3 Fiber breakage (Hashin's fiber failure initiation criterion [8]) The failure breakage occurs if the following equation is reached:

$$D_f = \frac{\sigma_{11}}{[\sigma_{11}]} \geq 1, (\sigma_{11} \geq 0) \qquad (3)$$

2.1 Validation and exploitation of the simulation

2.3.1 For an impact energy of 0.037 J

Vertical displacement amplitudes in this simulation and in the experiment are similar (0.38 mm for the simulation and 0.31mm for the experiment [2]).

2.3.2 For an impact energy of 0.3 J

The simulation curve evolution in this paper (Figure 5) and in R.K. Luo et al.'s paper [3] (Error! Reference source not found.) are reasonably similar. The first peak of the Figure 3 curve doesn't appear in the simulation curve. But it may be caused by an insufficient number of points in this paper simulation. The highest value of the normal stress σ22 is reached at about 0.3 ms (second peak) and values are stable between the two peaks for both the experiment and this simulation. The little difference in time may be explained by an offset in the time origin between the two simulations.

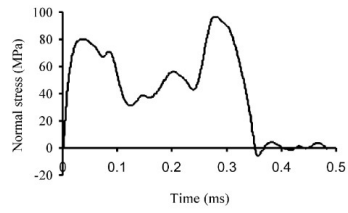

Fig.4 Dynamic response curve σ22 under 0.3 J impact for [04/904]s from R.K. Luo et al. [3]

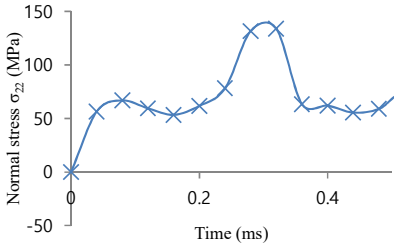

Fig. 5 Dynamic response curve σ22 under 0.3 J for $[0_4/90_4]_s$

The maximum value of the shear stress is 50 MPa for the figure 6 curve and is about 33 MPa for this paper simulation. This value is reached at 0.28 ms in R.K. Luo et al.'s simulation and at 0.31 ms in this simulation. The Figure 5 first peak doesn't appear in the simulation. A possible reason was described above. Moreover, the curve doesn't fall to zero after the 0.3 ms peak for this paper simulation contrary to the R.K. Luo et al.'s simulation.

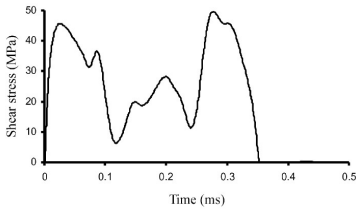

Fig. 6 Dynamic response curve τ_{13} under 0.3 J impact for $[0_4/90_4]_s$ from R.K. Luo et al. [3]

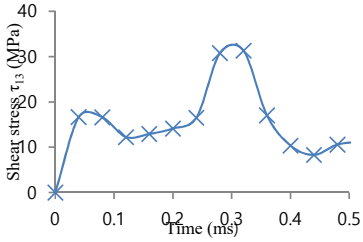

Fig. 7 Dynamic response curve σ13 under 0.3 J for $[0_4/90_4]_s$

Assuming that the simulation proposed by R.K. Luo et al. gives a good description of experiments (see [3] for the validation of this model), the simulation proposed in this paper was validated. Differences in results between the two simulations could be explained by the used elements.

2.3.3 For an impact energy of 0.59 J

To determine if the criteria (Equations (1), (2) et (3)) were reached, values of σ_{11}, σ_{22}, α_{33}, τ_{12}, τ_{13} and τ_{23} were picked up point by point. Criteria make sense if the values are picked in the same point. But, even if values were picked up for the same distance from the center of impact, the height and the direction in plate plane varied from one quantity to another to maximize all quantities and obtain qualitative results of criteria in order to know the damaged area dimensions.

No fiber breakage has been found in the finite element simulation. This is consistent with the experiment and with R.K. Luo et al.'s simulation. However, the results are different than R.K. Luo et al.'s results. A comparison is given in Table 2 for the $[0_4/90_4]_s$ plate.

Table 2 Result comparison for the $[0_4/90_4]_s$

Name	Matrix failure length (mm)
R.K. Luo's Experiment	17
R.K. Luo et al.'s simulation	13
This simulation	10.0±1.0

Note that lengths given in Table 2 are the half of the whole length because only one quarter of the plate was considered.

Differences in table 2 are not negligible. They may be ameliorated by using another method to calculate damage criteria. Picking up values point by point is not very easy but it could be possible to increase the number of points and to compare values in a same point and not for a same distance to center of impact. Moreover, a subroutine may be incorporated with the finite element package. Furthermore, results can be used to qualitatively compare the damage length with the orientation of the middle layer α.

2.2 Stacking sequence optimization

2.4.1 Method presentation and validation for an impact energy of 0.59 J

For α = 45, 90°, the previous model was kept because of the symmetry. For α = 15, 30, 60°, the entire plate was modeled as a shell and with cohesive elements [9]. A zero-thickness plate with radius of 10 mm (impactor radius was 5 mm) was used for modeling the cohesive layer. In order not to affect the final convergent results of the whole model and cause deflected behaviors, appropriate material properties were assigned to this plate (Table 3).

Table 3 Cohesive layer properties [5]

stiffness normal- mode K_{nn}	10^6 N/mm^3
Stiffness- first direction K_{ss}	10^6 N/mm^3
Stiffness second direction - K_{tt}	10^6 N/mm^3
Nominal stress normal-only mode (**Quads damage**)	61 MPa
Nominal stress first direction (**Quads damage**)	68 MPa
Nominal stress second direction (**Quads damage**)	68 MPa
Normal mode fracture energy	0.02 J/mm
Shear mode fracture energy first direction	0.2 J/mm
Shear mode fracture energy second direction	0.2 J/mm

Different stacking sequences were tested for different levels of energy to find out the best fiber direction against impact. The staking sequences were $[0_4/90_4]_s$, $[0_4/60_4]_s$, $[0_4/45_4]_s$, $[0_4/30_4]$s and $[0_4/15_4]_s$ (global notation $[0_4/\alpha_4]_s$). A concentrated mass of 1.60x10-2 kg was applied at the point of impact.

To validate the model, the shape of damages was compared with experimental and simulation results of previous works from R.K. Luo et al. [2,3] and from F. Aymerich et al. [4]; A peanut shape along the lower interface fiber orientation was found like in the previous works (Figure 8-9).

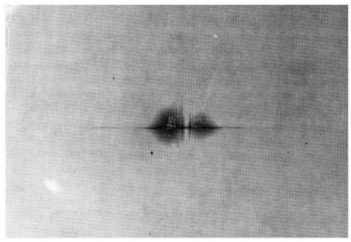

Fig. 8 X-ray photo showing the damage in a composite plate [3]

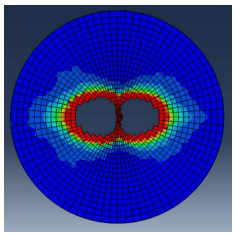

Fig. 9 Delamination criterion between 90_8 and 0_4 layers

2.4.2 Exploitation for an impact energy of 0.59 J

The results obtained for the different fiber stacking sequences are given in Figure 10 (note that the damage length is the half of the entire length because of the symmetry). The delamination was shown independent of the middle layer orientation.

For a 0.59 J impact, it was also shown that the matrix crack length is maximum for $\alpha = 45°$ and minimum for $\alpha = 90°$ (but the difference with $\alpha = 15°$ and with $\alpha = 30°$ is little). So, to optimize the plate properties, the [04/454]s has to be avoided and [04/904]s should be chosen.

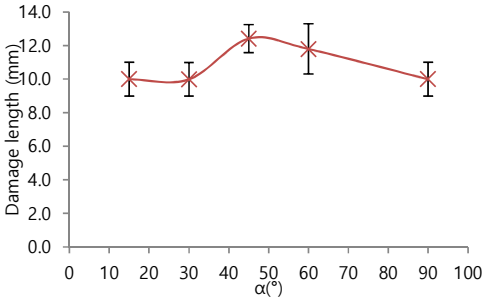

Fig. 10 Damage length by middle layer orientation (0.59 J)

2.4.3 Exploitation for an impact energy of 1.96 J

Other simulations were carried out with shell elements.

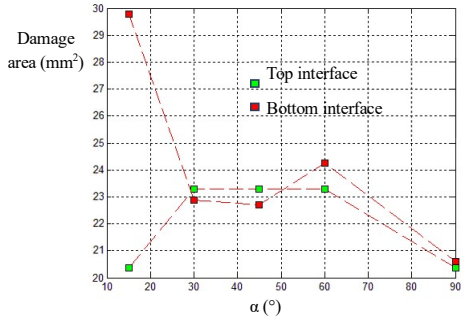

Fig. 11 Damage area by fiber stacking sequence (1.96J) [6]

Results for a 1.96 J impact are given in **Error! Reference source not found.**Figure 11. [04/904]s had the smallest damaged area, nearly 20.6 mm2 for the bottom 90°/0° interface and 20.35 mm2 for the top interface. For a higher level of the impact energy, it was again showed that the $[0_4/90_4]_s$ should be chosen.

3. Conclusions

This approach permits to compare the layer orientation angle effects on damaged area dimensions. It can predict whether the composite structure is damaged. For 0.59 J impact simulations, the damage has been identified as delamination coupled with matrix failure and no fiber breakage found, which has been validated by the experiment of R.K. Luo et al. However, it cannot quantitatively predict the dimensions of the damaged area. To make this approach easier to use and to improve results, it is possible to create and incorporate a subroutine with the finite element package.

REFERENCES

1. Gholizadeha S., Review of Impact Behaviour in Composite Materials, International Journal of Mechanical and Production Engineering, Vol. 7, 3 (2019), pp. 35-46
2. Luo R.K., Green E.R., Morrison C.J., "Impact damage analysis of composite plates," International Journal of Impact Engineering, vol. 22, pp. 435-447, 1999.
3. Luo R.K., Green E.R., Morrison C.J., "An approach to evaluate the impact damage initiation and propagation in composite plates," *Composites: Part B*, vol. 32, pp. 513-520, 2001.
4. Aymerich F., Dore F., Priolo P., "Prediction of impact-induced delamination in cross-ply composite laminates using cohesive interface elements," Composites Science and Technology, vol. 68, pp. 2383-2390, 2008.
5. Nguyen Duc Anh, Nguyen The Hoang (2010), "Low-energy impact behaviour of laminated composite," Ho Chi Minh City University of Technology .
6. Nguyen Van Anh Tuan, Nguyen The Hoang (2012), "Predicting Impact Behaviour on Composite Laminate," Ho Chi Minh City University of Technology .
7. Dreamliner Boeing 787 Specs, 2015 [Online]. Available: https://modernairliners.com/boeing-787-dreamliner/boeing-787-dreamliner-specs/
8. Hashin Z., Failure criteria for unidirectional fiber composites, Journal of Applied Mechanics, Vol. 47, 2 (1980), pp. 329–334.
9. Hibbitt, Karlsson, and Sorensen (1998). ABAQUS Theory manual 5.8.